



Molecular Crystals and Liquid Crystals Science and Technology. Section A. Molecular Crystals and Liquid Crystals

Publication details, including instructions for authors and subscription information:

<http://www.tandfonline.com/loi/gmcl19>

Electric and Magnetic Properties of the Radical Salts $\text{ET}_5[\text{B}_{10}\text{I}_{10}] \cdot (\text{CH}_2\text{Cl}_2)_{0.8}$ and $\text{ET}_{11}[\text{P}_2\text{W}_{18}\text{O}_{62}] \cdot 3\text{H}_2\text{O}$

Carlos Gimenez-saiz^a, J. Derek Woollins^a,
Alexandra M. Z. Slawin^a, Eugenio Coronado^b, Jose
M. Martinez-agudo^b, Carlos J. Gomez-garcia^b &
Neil Robertson^c

^a Department of Chemistry, Loughborough Univ.,
Loughborough, LE11 3TU, UK

^b Departamento de Química Inorgánica, Univ. de
Valencia, Dr. Moliner, 50, E-46100, Burjassot, (Spain)

^c Department of Chemistry, Univ. of Edinburgh, West
Mains Road, Edinburgh, EH9 3JJ, UK

Version of record first published: 24 Sep 2006

To cite this article: Carlos Gimenez-saiz, J. Derek Woollins, Alexandra M. Z. Slawin, Eugenio Coronado, Jose M. Martinez-agudo, Carlos J. Gomez-garcia & Neil Robertson (1999): Electric and Magnetic Properties of the Radical Salts $\text{ET}_5[\text{B}_{10}\text{I}_{10}] \cdot (\text{CH}_2\text{Cl}_2)_{0.8}$ and $\text{ET}_{11}[\text{P}_2\text{W}_{18}\text{O}_{62}] \cdot 3\text{H}_2\text{O}$, Molecular Crystals and Liquid Crystals Science and Technology. Section A. Molecular Crystals and Liquid Crystals, 335:1, 43-52

To link to this article: <http://dx.doi.org/10.1080/10587259908028850>

PLEASE SCROLL DOWN FOR ARTICLE

Full terms and conditions of use: <http://www.tandfonline.com/page/terms-and-conditions>

This article may be used for research, teaching, and private study purposes. Any substantial or systematic reproduction, redistribution, reselling, loan, sub-licensing, systematic supply, or distribution in any form to anyone is expressly forbidden.

The publisher does not give any warranty express or implied or make any representation that the contents will be complete or accurate or up to date. The accuracy of any instructions, formulae, and drug doses should be independently verified with primary sources. The publisher shall not be liable for any loss, actions, claims, proceedings, demand, or costs or damages whatsoever or howsoever caused arising directly or indirectly in connection with or arising out of the use of this material.

Electric and Magnetic Properties of the Radical Salts $\text{ET}_5[\text{B}_{10}\text{I}_{10}] \cdot (\text{CH}_2\text{Cl}_2)_{0.8}$ and $\text{ET}_{11}[\text{P}_2\text{W}_{18}\text{O}_{62}] \cdot 3\text{H}_2\text{O}$

CARLOS GIMENEZ-SAIZ^a, J. DEREK WOOLLINS^a, ALEXANDRA M.Z. SLAWIN^a, EUGENIO CORONADO^b, JOSE M. MARTINEZ-AGUDO^b, CARLOS J. GOMEZ-GARCIA^b and NEIL ROBERTSON^c

^a*Department of Chemistry, Loughborough Univ., Loughborough, LE11 3TU UK,* ^b*Departamento de Química Inorgánica, Univ. de Valencia, Dr. Moliner, 50, E-46100 Burjassot (Spain) and* ^c*Department of Chemistry, Univ. of Edinburgh, West Mains Road, Edinburgh, EH9 3JJ UK*

The magnetic and electrical characterization of the radical salts formed by the organic donor bis(ethylenedithio)tetrathiafulvalene (abbreviated to ET) and the large inorganic clusters $[\text{B}_{10}\text{I}_{10}]^{2-}$ and $[\text{P}_2\text{W}_{18}\text{O}_{62}]^{6-}$ are presented.

Keywords: magnetic measurements; conductivity; organic conductors based on radical cations; organic/inorganic structures

INTRODUCTION

Radical salts of the donor ET (Fig. 1a) exhibit many different structural arrangements of the organic component giving rise to a large variety of electronic structures from insulators to metallic conductors and superconductors in low-dimensional frameworks.⁽¹⁾ These organic materials have interesting

features of electrical and magnetic properties depending mainly on the structure and band filling of the organic donors, which are induced by the anions.

In order to look for novel structural packings in the organic sublattice (and hence new electronic properties), we are investigating the use of anionic clusters with large sizes as the inorganic components of cation radical salts.

Two kinds of inorganic anions which have already been used for this purpose are the boranes^[2] and the polyoxometalates,^[3] giving rise to radical salts showing various molecular stacking patterns different from those obtained with simple anions, such as Cl^- , I_3^- , BF_4^- or PF_6^- .

A particular characteristic of boranes is their chemical versatility, which permits the incorporation of a diversity of organic and inorganic functional groups to their molecular structure. This can be exploited in the design of radical cation salts by using boranes with functional groups or atoms which can interact with the organic donors, for example hydrogen bond formation with the ethylene groups of ET. With this aim we have used the borane anion $[\text{B}_{10}\text{I}_{10}]^{2-}$ (Fig. 1b) as the inorganic component of new radical cation salts.

Moreover, we have recently reported the first radical salt containing a Dawson-Wells polyoxometalate,^[4] $\text{ET}_{11}[\text{P}_2\text{W}_{18}\text{O}_{62}]\cdot 3\text{H}_2\text{O}$, (Fig. 1c) which presents several unusual structural features. We present here the magnetic characterization of this radical salt.

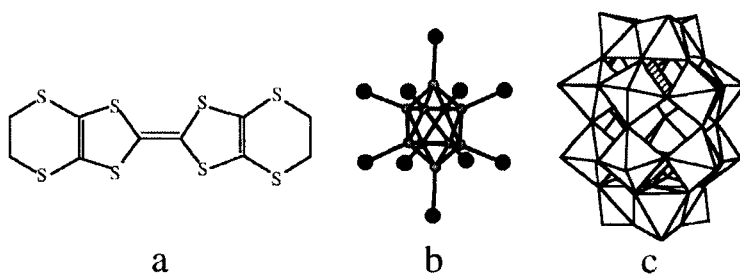


FIGURE 1 Molecules used in this work: (a) the donor ET; (b) the anion $[\text{B}_{10}\text{I}_{10}]^{2-}$; (c) the Dawson-Wells polyoxoanion $[\text{P}_2\text{M}_{18}\text{O}_{62}]^{6-}$ (M = Mo, W).

RESULTS AND DISCUSSION

By reaction of the well-known borane anion $[\text{B}_{10}\text{H}_{10}]^{2-}$ with Cl_2 , Br_2 or I_2 it is possible to obtain the series of halogenated borane clusters $[\text{B}_{10}\text{X}_{10}]^{2-}$ ($\text{X} = \text{Cl}, \text{Br}, \text{I}$),^[5] in which the halogen atoms are situated in the periphery of the anions (Fig. 1b). In contrast, the polyoxometalate $[\text{P}_2\text{W}_{18}\text{O}_{62}]^{6-}$ exhibits the so-called Dawson-Wells structure (Fig. 1c) in which 18 octahedra $[\text{WO}_6]$ are sharing edges and corners leaving two tetrahedral cavities inside which are occupied by P^{V} atoms. The external appearance of this anion shows two belts of six octahedra capped by two groups of three octahedra sharing edges.

The radical salt $\text{ET}_5[\text{B}_{10}\text{I}_{10}] \cdot (\text{CH}_2\text{Cl}_2)_{0.8}$

By electro-oxidation of the organic donor ET at low constant current (0.5 μA) in the presence of a solution (1:1 mixture of $\text{CH}_3\text{CN}/\text{CH}_2\text{Cl}_2$) containing the borane anion $[\text{B}_{10}\text{I}_{10}]^{2-}$ we have obtained single crystals of the new radical salt $\text{ET}_5[\text{B}_{10}\text{I}_{10}] \cdot (\text{CH}_2\text{Cl}_2)_{0.8}$ (Fig. 2). Its structure (space group $\text{P}2_1/\text{c}$ with $a = 22.8678(9)$, $b = 24.2251(10)$, $c = 20.5168(8)$, $\beta = 112.691(1)$ and $V = 10486.1 \text{ \AA}^3$) consists of alternating layers of organic donors and inorganic anions. The organic layers are formed by infinite parallel chains of ET molecules that accommodate between the layers of large anions by stacking in a zigzag mode (Fig. 2a). The ET molecules of neighboring chains are also parallel, giving rise to the so-called β phase (Fig. 2b). In the organic layer there are five crystallographically independent ET molecules, labeled A, B, C, D and E, that are ordered in all chains following the same sequence (...ABCDE...), although the direction of the sequence is not always the same in all chains: two neighboring chains with the same direction of the sequence alternate with two other chains exhibiting the sequence in the opposite direction, as can be seen in Fig. 2b.

From the crystallographic data, using the known correlations between the intramolecular bond distances and the degree of ionicity,^[6] we can roughly estimate that C and D type molecules are almost completely ionized whereas A,

B and E molecules are close to neutral. This charge distribution is consistent with the structural differences shown by the ET molecules. Thus A, B and E molecules show clear distortions with respect to the planarity which can be associated with a neutral state, while C and D molecules are almost planar.

As in other two-dimensional ET salts, the shortest interchain S...S distances (ranging from 3.32 to 3.64 Å) are shorter than the intrachain ones (ranging from 3.53 to 3.78 Å). Moreover, in this salt containing the $[B_{10}I_{10}]^{2-}$ anion, there are several short C-H...I contacts which we consider to be C-H...I hydrogen bonds. Every ET molecule forms hydrogen bonds using the ethylene groups of both sides of the molecule (the distances C-H...I range from 2.98 to 3.39 Å). In particular, some of the terminal ethylene groups of the A, B and E types molecules markedly bend towards the iodine atoms of $[B_{10}I_{10}]^{2-}$ (see Fig. 2a), explaining the conformations adopted by these ethylene groups.

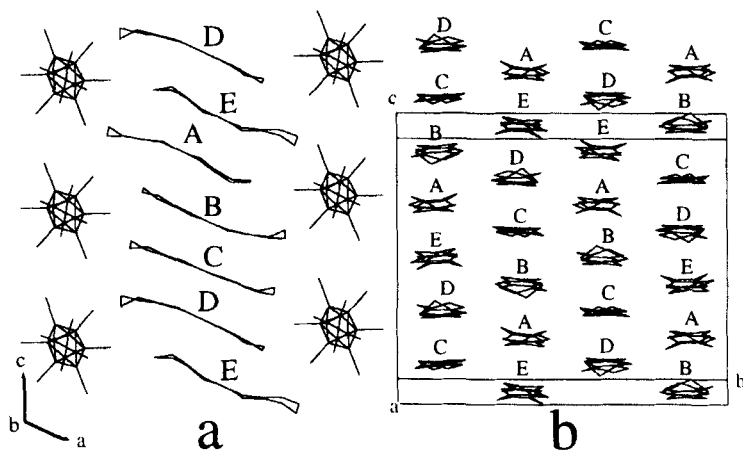


FIGURE 2 (a) View of one zigzag chain of ET molecules along the c direction; (b) view of the ET molecules forming the β phase (bc plane).

Conductivity measurements made using the four contacts method along the best developed dimension of the needle-like single crystals of this radical salt show a conductivity of $1.1 \cdot 10^{-3} \text{ S} \cdot \text{cm}^{-1}$ at room temperature, and the thermal dependence indicates a semiconducting behavior with an activation energy of 156 meV (Fig. 3).

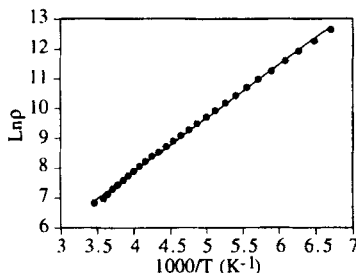


FIGURE 3 Plot of the logarithm of the dc resistivity (in $\Omega \text{ cm}$) versus reciprocal temperature for $\text{ET}_5[\text{B}_{10}\text{I}_{10}] \cdot (\text{CH}_2\text{Cl}_2)_{0.8}$. The solid line is the linear fit.

The magnetic properties of this salt have been investigated in the temperature range 2-300 K at a magnetic field of 1 T, using a SQUID susceptometer. The results are displayed in Fig. 4. The $\chi_m T$ product at room temperature is about $0.80 \text{ emu} \cdot \text{T} \cdot \text{mol}^{-1}$, which is very close to the calculated value of 0.75 expected for two non-interacting electrons in the organic sublattice, since the $[\text{B}_{10}\text{I}_{10}]^{2-}$ anion is diamagnetic. As the temperature is lowered, the $\chi_m T$ product shows a gradual decrease, approaching zero at low temperatures. Such a behavior of the magnetic moment can be attributed to antiferromagnetic interactions in the organic part. In fact, the susceptibility vs. T plot (Fig. 4b) presents a maximum at about 110 K, confirming the existence of antiferromagnetic interactions and a Curie-like tail at low temperatures, suggesting the presence of monomeric impurities coming from isolated ET^+ molecules. As can be seen in Fig. 2b, C and D type molecules (the ones which

are completely ionized) are adjacent in the sequence of ET molecules that form the organic stacks, forming dimers that are separated by neutral ET molecules. Then, a model of antiferromagnetically coupled dimers would be a reasonable description for the magnetic data. Accordingly, we have fitted the experimental data to a model of antiferromagnetically coupled dimers with a Curie-like contribution coming from the isolated ET^+ molecules (Equation 1, in which J and θ are the intra and interdimer exchange parameters respectively).

$$\chi_m = \left(\frac{3g^2}{4T} \right) \left(\frac{T}{T - \theta} \right) \left(\frac{1}{3 + \exp(-J/T)} \right) + \frac{C}{T} \quad (1)$$

This model reproduces very satisfactorily the high temperatures region (solid line in Fig. 4b) with J , θ and C values of -128.8 cm^{-1} , -95.4 cm^{-1} and $0.0716 \text{ emu.K.mol}^{-1}$, respectively (g has been fixed to 2). However, it is not able to reproduce the low temperatures region, suggesting that there must be an extra contribution and, therefore, an additional *inter-dimers* coupling must be considered. Band structure calculations which would permit an estimation of the transfer integrals are planned, in order to confirm this possibility.

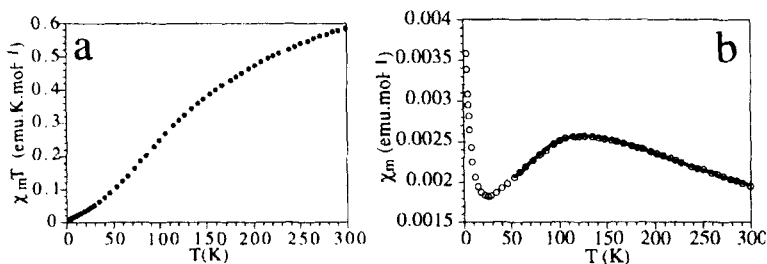


FIGURE 4 Magnetic behavior of the $\text{ET}_5[\text{B}_{10}\text{I}_{10}]\cdot(\text{CH}_2\text{Cl}_2)_{0.8}$ salt.

The salt $\text{ET}_{11}[\text{P}_2\text{W}_{18}\text{O}_{62}]\cdot 3\text{H}_2\text{O}$

The structure of the radical salt $\text{ET}_{11}[\text{P}_2\text{W}_{18}\text{O}_{62}]\cdot 3\text{H}_2\text{O}$ has been previously reported^[4] and shows some resemblance with the structure of the $\text{ET}_5[\text{B}_{10}\text{I}_{10}]$ salt. For example, the organic molecules form layers exhibiting the β phase and are formed by zigzag chains of ET molecules (Fig. 5). In this case, we find up to 6 crystallographically independent ET molecules (labeled as A, B, C, D, E and F), that follow the sequence ...ABCDEFEDCBA... in all chains. No differences in the direction of the sequence are found here.

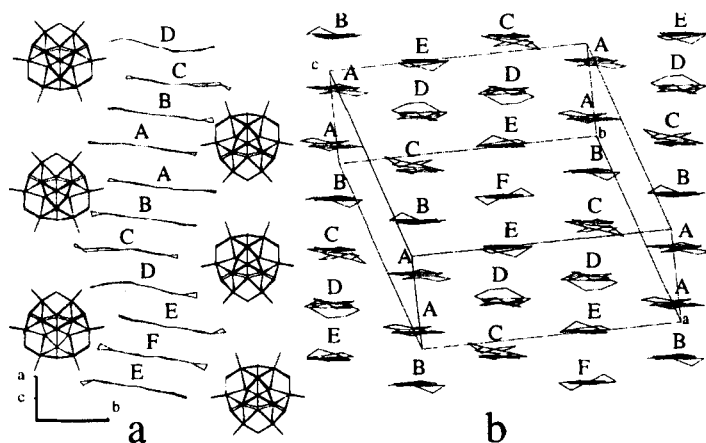


FIGURE 5 $\text{ET}_{11}[\text{P}_2\text{W}_{18}\text{O}_{62}]\cdot 3\text{H}_2\text{O}$: (a) View of one zigzag chain of ET molecules along the [401] direction and (b) projection of the structure in the ac plane showing the β packing.

The conductivity of a single crystal measured using the four contacts method shows an increase from ca. $5 \text{ S}\cdot\text{cm}^{-1}$ at 298 K to $5.5 \text{ S}\cdot\text{cm}^{-1}$ at 230 K (Fig. 6a). Below this temperature the conductivity decreases as the temperature is lowered, after a very broad transition of metal-insulator type. This kind of behavior suggests that this salt is a semiconductor with a very small energy

gap. Epstein *et al.*^[17] have proposed a model to explain the electrical behavior of such semiconducting radical salts by using Equation 2, in which E_a is the activation energy and A and α are constant parameters.

$$\sigma = A T^{-\alpha} e^{-E_a/kT} \quad (2)$$

Using this equation, we fit the electric behavior of this salt (solid line in Fig. 6a) and find values of $A = 22006 \Omega^{-1}\text{cm}^{-1}$, $\alpha = 1.28$ and $E_a = 27 \text{ meV}$. The value of the activation energy is one order of magnitude lower than those found in radical salts of the donor ET with other polyoxometalates,^[3b] accounting for the higher conductivity at room temperature of the salt $\text{ET}_{11}[\text{P}_2\text{W}_{18}\text{O}_{62}]\cdot 3\text{H}_2\text{O}$.

The single crystal ESR measurements show a lorentzian line with $g \approx 2$ and a line width of 13-19 G for any direction of the magnetic field except when it is in the *ac* plane where a dysonian line with $A/B \approx 1.6$ can be observed at 300 K. The g values are typical of these kind of radical salts. The line width values are comparable to those found in other β phases^[1] and decrease as the temperature is lowered. The magnetic susceptibility of this salt was measured using a SQUID susceptometer in the temperature range 2-300 K at an applied magnetic field of 1 T. The χ_m vs. T plot is displayed in Fig. 6b. The value of χ_m is around $0.006 \text{ emu}\cdot\text{mol}^{-1}$ at 300 K, indicating the presence of almost 6 electrons in the organic sublattice (the $[\text{P}_2\text{W}_{18}\text{O}_{62}]^{6-}$ anion is diamagnetic). When the temperature decreases the susceptibility remains constant down to 50 K. Below this temperature χ_m exponentially increases. This behavior is indicative of a weak Pauli paramagnetism (accounting for the constant values at high temperatures) and a paramagnetic tail (responsible for the slope at low temperatures). Thus, we fit the magnetic susceptibility to Equation 3.

$$\chi_m = N\alpha + C/T \quad (3)$$

The value of the Pauli paramagnetism so obtained ($N\alpha = 5.42(2) \cdot 10^{-3} \text{ emu.mol}^{-1}$) is close to the values observed for other radical salts with metallic behavior or high conductivity.^[1] Likewise, the value of the Curie tail ($C = 0.0247(1) \text{ emu.K.mol}^{-1}$) is slightly lower than the corresponding values found in the radical salts formed by ET and Keggin-type polyoxometalates.^[3b] The value of the Curie tail can be explained assuming the presence of magnetic impurities in the form of isolated ET molecules having a degree of ionicity of +1, the calculated percentage of these ionized molecules being around 10%.

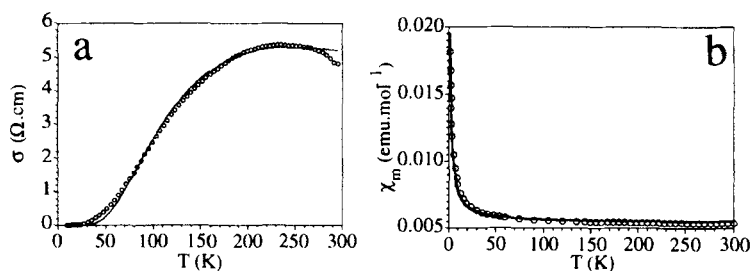


FIGURE 6 (a) Electric conductivity vs. T in the ac crystallographic plane of a single crystal of $\text{ET}_{11}[\text{P}_2\text{W}_{18}\text{O}_{62}] \cdot 3\text{H}_2\text{O}$. The solid line represents the best fit to Equation 2. (b) χ_m vs. T plot for the salt $\text{ET}_{11}[\text{P}_2\text{W}_{18}\text{O}_{62}] \cdot 3\text{H}_2\text{O}$. The solid line represents the best fit to Equation 3.

CONCLUSIONS

We have shown in this contribution two examples of organic/inorganic hybrid materials in which the use of bulky inorganic anions induce unusual

structural packings in the organic sublattice. In both cases there is a high number of crystallographically independent ET molecules (5 and 6) forming exotic zigzag chains and, in the case of the Dawson-Wells polyoxoanion, it has led to the highest donor to anion ratio (11:1) in a radical salt of the ET donor. In the $[\text{B}_{10}\text{I}_{10}]^{2-}$ salt the ethylene groups of the ET molecules bend towards the iodine atoms of the anion in order to form the maximum number of hydrogen bonds. From the physical point of view, the $\text{ET}_5[\text{B}_{10}\text{I}_{10}]$ is a semiconductor due to the existence of dimers of fully ionized ET molecules. The magnetic properties indicate that these dimers are not isolated (as could be expected from the structural data). Band structure calculations are in progress to determine the interaction model between these dimers. The salt $\text{ET}_{11}[\text{P}_2\text{W}_{18}\text{O}_{62}]\cdot 3\text{H}_2\text{O}$ shows a metallic-like behavior at high temperatures, opening the way for the synthesis of metallic salts with magnetic character by replacing one of the W atoms of the Dawson-Wells anion by magnetic transition metals.

Acknowledgments

The authors thank the support of the COST Action 518 (Project on Magnetic Properties of Molecular and Polymeric Materials).

References

- [1] J.M. Williams, J.R. Ferraro, R.J. Thorn, K.D. Carlson, U. Geiser, H. H. Wang, A.M. Kini, and M.H. Whangbo, *Organic Superconductors, Synthesis, Structure, Properties and Theory* (Ed.: R. N. Grimes), Prentice Hall, Englewood Cliffs, New Jersey, (1992).
- [2] Y.K. Yan, D.M.P. Mingos, *Chem. Soc. Rev.*, 203 (1995) and references therein.
- [3] For radical salts with polyoxometalates see: (a) L. Ouahab, *Chem. Mater.*, **9**, 1909 (1997) and references therein. (b) E. Coronado, C.J. Gómez-García, *Chem. Rev.*, **98**, 273 (1998) and references therein.
- [4] E. Coronado, J.R. Galán Mascarós, C. Giménez-Saiz, and C.J. Gómez-García, *Advanced Materials*, **8**, 801 (1996).
- [5] W.H. Knoch, H.C. Miller, J.C. Sauer, J.H. Balthis, Y.T. Chia, and E. L. Muetterties, *Inorg. Chem.*, **3**, 159 (1964).
- [6] P. Guionneau, C.J. Kepert, G. Bravic, D. Chasseau, M.R. Kurmoo, P. Day, *Synth. Met.*, **86**, 1973 (1997).
- [7] (a) J.S. Miller, A.J. Epstein, *Angew. Chem. Int. Ed. Engl.*, **26**, 287 (1987). (b) A.J. Epstein, E.M. Conwell, D.J. Sandman, J.S. Miller, *Solid State Commun.*, **23**, 355 (1977).